Full Paper

CSIRO PUBLISHING

Aust. J. Chem. **2010**, *63*, 1448–1452

www.publish.csiro.au/journals/ajc

Complexation of Zn^{2+} by the Fluorophore 2-((*E*)-2-Phenyl) ethenyl-8-(*N*-4-methylbenzenesulfonyl)aminoquinol-6-yloxyacetic Acid: A Preparative, Potentiometric, UV-visible, and Fluorescence Study

Hilary C. Coleman,[A] *Bruce L. May,*[A] *and Stephen F. Lincoln*[A,B]

[A]School of Chemistry and Physics, University of Adelaide, Adelaide, SA 5005, Australia.
[B]Corresponding author. Email: Stephen.Lincoln@adelaide.edu.au

The preparation of the Zn^{2+} specific fluorophore 2-((*E*)-2-phenyl)ethenyl-8-(*N*-4-methylbenzene-sulfonyl)aminoquinol-6-yloxyacetic acid, $H_2\mathbf{3}$, is described. The protonated form, $H_3\mathbf{3}^+$, is characterized by pK_a values of 2.71 ± 0.03, 4.92 ± 0.03, and 10.46 ± 0.03 in 25% (v/v) aqueous ethanol 0.10 mol L^{-1} in $NaClO_4$ at 298.2 K determined by potentiometric titration. At pH 6.6, but otherwise under the same conditions, the dianion, $\mathbf{3}^{2-}$, forms the fluorescent complexes [Zn(**3**)] and $[Zn(\mathbf{3})_2]^{2-}$, characterized by $\log(K_1/L\,mol^{-1}) = 10.5 \pm 0.20$ and $\log(K_2/L\,mol^{-1}) = 11.1 \pm 0.1$, respectively, as determined by fluorimetry. These data are compared with analogous data for the structurally similar and widely used fluorophore 2-methyl-8-*p*-toluenesulfonamido-6-quinolyloxyacetic acid (Zinquin A).

Manuscript received: 28 April 2010.
Manuscript accepted: 1 July 2010.

Introduction

Zinc(II) is the second most abundant transition metal ion in humans after Fe^{2+}/Fe^{3+}.[1–3] It is involved in many physiological processes and is largely found either at the active site or as a structural component of numerous enzymes.[4–8] Zinc(II) regulates RNA and DNA metabolism[9–11] and some neurological diseases appear to involve Zn^{2+} metabolic dysfunction.[12–14] Consequently, the location and quantification of Zn^{2+} in biological tissues is of significant importance and has led to the development of a substantial range of ligands which fluoresce when bound by Zn^{2+}.[14–18]

The tissue stain 8-aminoquinoline, **1** (Fig. 1), was the starting point for the development of the widely used Zn(II) specific fluorophore, 2-methyl-8-*p*-toluenesulfonamido-6-quinolyloxyacetic acid, $H_2\mathbf{2}$, and its ethyl ester (Zinquin A and E)[15,18–26] and we now report a study of the styryl derivative of $H_2\mathbf{2}$, 2-((*E*)-2-phenyl)ethenyl-8-(*N*-4-methylbenzenesulfonyl)aminoquinol-6-yloxyacetic acid, $H_2\mathbf{3}$, as part of a broad study of the effect of ligand structural change on the formation of Zn^{2+} complexes, and the potential for development of new Zn^{2+} selective fluorophore designs.

Results and Discussion

Potentiometric Determination of the pK_as of $H_3\mathbf{3}^+$

2-((*E*)-2-Phenyl)ethenyl-8-(*N*-4-methylbenzenesulfonyl)aminoquinol-6-yloxyacetic acid, $H_2\mathbf{3}$, was prepared by the hydrolysis of its ethyl ester.[27] Potentiometric titrations of 1.03×10^{-3} mol L^{-1} $H_2\mathbf{3}$ in 25% v/v aqueous ethanol in the presence of 9.2×10^{-3} mol L^{-1} $HClO_4$ at $I = 0.10$ mol L^{-1} ($NaClO_4$) with 0.126 mol L^{-1} NaOH at 298.2 K, show $H_3\mathbf{3}^+$ to undergo three acid dissociations characterized by $pK_{a3} = 10.46 \pm 0.03$, $pK_{a2} = 4.92 \pm 0.03$, and $pK_{a1} = 2.71 \pm 0.03$, which are assigned to the sulfonamide, carboxylic, and quinolinium protons, respectively. These compare with $pK_{a3} = 10.13 \pm 0.08$, $pK_{a2} = 4.40 \pm 0.02$, and $pK_{a1} = 3.08 \pm 0.06$ for $H_3\mathbf{2}^+$ under the same conditions.[15b] Thus, the quinolinium

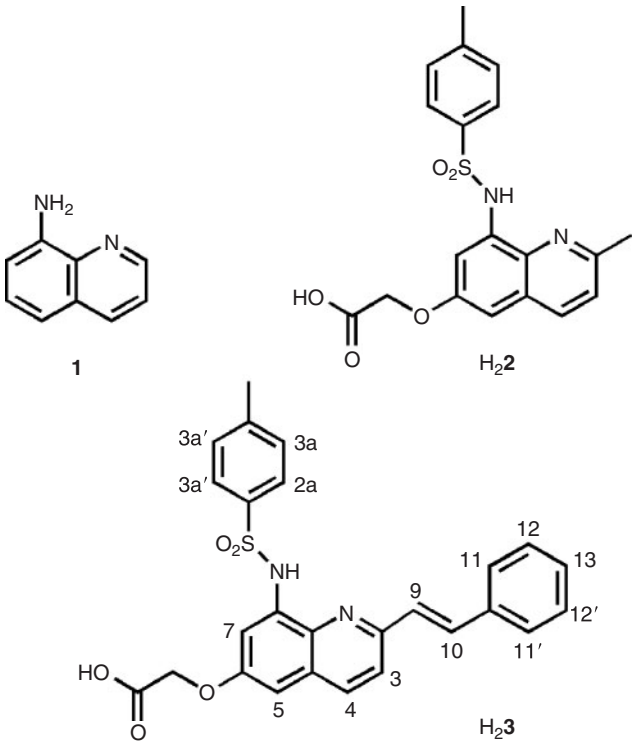

Fig. 1. Structures of **1**, $H_2\mathbf{2}$, and $H_2\mathbf{3}$.

10.1071/CH10173 0004-9425/10/101448

proton of $H_3\mathbf{3}^+$ is more acidic than that of $H_3\mathbf{2}^+$, while the sulfonamide and carboxylic protons are less acidic. This is consistent with the increased conjugation destabilizing $H_2\mathbf{3}^+$ with respect to $H_2\mathbf{3}$ to a greater extent than the destabilization of $H_3\mathbf{2}^+$ with respect to $H_2\mathbf{2}$. The higher pK_{a2} and pK_{a3} characterizing $H_2\mathbf{3}$ and $H\mathbf{3}^-$, respectively, probably reflect the greater delocalization of the di- and mono-negative charges of their conjugate bases, $H\mathbf{3}^-$ and $\mathbf{3}^{2-}$, respectively, and decreased electrostatic resistance to deprotonation by comparison with $H_2\mathbf{2}$ and $H\mathbf{2}^-$.

*UV-visible Studies of [Zn(**3**)] and [Zn(**3**)$_2$]$^{2-}$ Formation*

UV-vis spectra were recorded for 25% v/v aqueous ethanol solutions buffered at pH 6.6 with 1.0×10^{-3} mol L^{-1} NaPIPES buffer at $I = 0.10$ mol L^{-1} ($NaClO_4$) and 298.2 K under which conditions the ligand exists dominantly as $H\mathbf{3}^-$. The variation of the UV-vis spectrum of $H\mathbf{3}^-$ with increasing $[Zn^{2+}]_{total}$ is shown in Fig. 2. The best fit of an algorithm for the equilibria shown in Eqns 1 and 2 to the absorbance variation at 1.0 nm intervals over the range 270–450 nm yields $\log(K_1/\text{L mol}^{-1}) = 11.5 \pm 0.76$ ($K_1 = 3.2 \times 10^{11}$ L mol^{-1}) and $\log(K_2/\text{L}^2\ \text{mol}^{-2}) = 9.7 \pm 0.84$ ($K_2 = 5.0 \times 10^9$ L mol^{-1}). The derived UV-vis spectrum of $H\mathbf{3}^-$ and those of [Zn(**3**)] and [Zn(**3**)$_2$]$^{2-}$ obtained from the fitting procedure are shown in Fig. 3 from which it is seen that the spectra of [Zn(**3**)] and [Zn(**3**)$_2$]$^{2-}$ are shifted to longer wavelengths by comparison with those of $H\mathbf{3}^-$ as a consequence of their greater conjugation. The corresponding UV-vis spectra of (a) $H\mathbf{2}^-$ ($\lambda_{max} = 245$ nm and $\varepsilon = 4.1 \times 10^4$ L mol^{-1} cm^{-1} and $\lambda_{max} = 336$ nm and $\varepsilon = 4.2 \times 10^3$ L mol^{-1} cm^{-1}); (b) [Zn(**2**)] ($\lambda_{max} = 264$ nm and $\varepsilon = 3.6 \times 10^4$ L mol^{-1} cm^{-1} and $\lambda_{max} = 361$ nm and $\varepsilon = 3.9 \times 10^3$ L mol^{-1} cm^{-1}); and (c) [Zn(**2**)$_2$]$^{2-}$ ($\lambda_{max} = 264$ nm and $\varepsilon = 9.3 \times 10^4$ L mol^{-1} cm^{-1} and $\lambda_{max} = 361$ nm and $\varepsilon = 7.8 \times 10^4$ L mol^{-1} cm^{-1}) are consistent with their lesser conjugation by comparison with $H\mathbf{3}^-$, [Zn(**3**)], and [Zn(**3**)$_2$]$^{2-}$, respectively, resulting in shorter λ_{max}.

$$H\mathbf{3}^{-1} + Zn^{+2} \leftrightarrow H^+ + [Zn(\mathbf{3})] \quad (1)$$

$$H\mathbf{3}^- + [Zn(\mathbf{3})] \leftrightarrow H^+ + [Zn(\mathbf{3})_2]^{2-} \quad (2)$$

*Fluorimetric Studies of [Zn(**3**)] and [Zn(**3**)$_2$]$^{2-}$ Formation*

Under the same conditions as those of the UV-vis studies the fluorescence of $H\mathbf{3}^-$ increases with increase in $[Zn^{2+}]_{total}$ as shown in Fig. 4. The best fit of an algorithm for the sequential equilibria represented by Eqns 1 and 2 to the fluorescence variation at 0.5 nm intervals over the range 430–650 nm yields $\log(K_1/\text{L mol}^{-1}) = 10.5 \pm 0.20$ ($K_1 = 3.2 \times 10^{10}$ L mol^{-1}) and $\log(K_2/\text{L mol}^{-1}) = 11.1 \pm 0.1$ ($K_2 = 1.3 \times 10^{11}$ L mol^{-1}). Because of the greater changes in the fluorescence spectra as $[Zn^{2+}]_{total}$ increases by comparison with the changes and in the UV-vis spectra and the greater wavelength range of 220 nm suitable for K_1 and K_2 derivation from the fluorescence data compared with the 180 nm wavelength range for the UV-vis data, the K_1 and K_2 obtained by fluorimetry are considered the more accurate. Their similar magnitudes are consistent with the coordination number of [Zn(**3**)] changing from six (where four aqua ligands share the first coordination sphere and $\mathbf{3}^{2-}$ is coordinated as a bidentate ligand through the sulfonamide and quinol nitrogens) to four in tetrahedral [Zn(**3**)$_2$]$^{2-}$ as a consequence of steric interactions between the two $\mathbf{3}^{2-}$ ligands and the coordinative and stereochemical flexibility of d^{10} Zn^{2+}. For [Zn(**2**)], $\log(K_1/\text{L mol}^{-1}) = 10.5$ and for [Zn(**2**)$_2$]$^{2-}$,

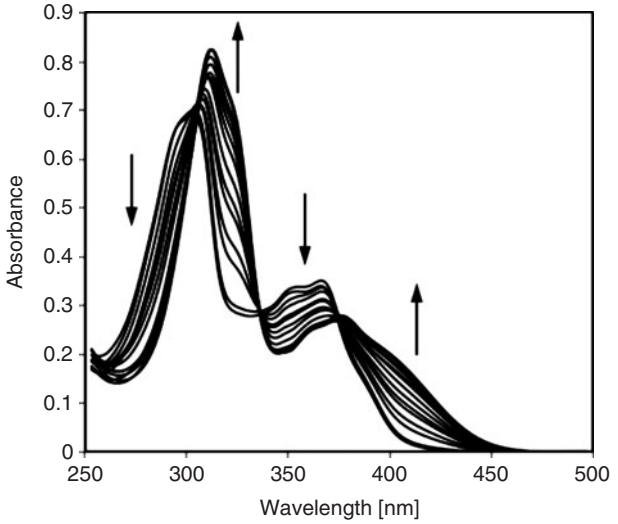

Fig. 2. Variation of the UV-vis spectrum of 1.82×10^{-5} mol L^{-1} $H\mathbf{3}^-$ in 25% v/v aqueous ethanol buffered 0.10 mol L^{-1} in $NaClO_4$ buffered at pH 6.6 (1.0×10^{-3} mol L^{-1} NaPIPES) at 298.2 K with $[Zn^{2+}]_{total}$ in the range 3.9×10^{-7} mol L^{-1} ($= [Zn^{2+}]_{adventitious}$) to 1.72×10^{-4} mol L^{-1}. The arrows show the direction of absorbance change with increase in $[Zn^{2+}]_{total}$. Isosbestic points occur at 305, 336, and 375 nm.

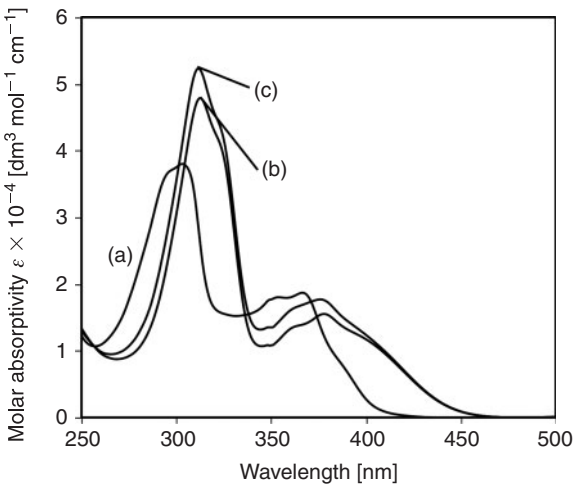

Fig. 3. The UV-vis spectra of (a) $H\mathbf{3}^-$ ($\lambda_{max} = 303$ nm and $\varepsilon = 3.8 \times 10^4$ L mol^{-1} cm^{-1} and $\lambda_{max} = 366$ nm and $\varepsilon = 1.9 \times 10^4$ L mol^{-1} cm^{-1}); (b) [Zn(**3**)] ($\lambda_{max} = 313$ nm and $\varepsilon = 4.8 \times 10^4$ L mol^{-1} cm^{-1} and $\lambda_{max} = 378$ nm and $\varepsilon = 1.5 \times 10^4$ L mol^{-1} cm^{-1}); and (c) [Zn(**3**)$_2$]$^{2-}$ ($\lambda_{max} = 312$ nm and $\varepsilon = 5.2 \times 10^4$ L mol^{-1} cm^{-1} and $\lambda_{max} = 376$ nm and $\varepsilon = 1.8 \times 10^4$ L mol^{-1} cm^{-1}) derived from the fitting of an algorithm for the molar absorbance variation with $[Zn^{2+}]_{total}$ and equilibria (1) and (2) as described in the text.

$\log(K_2/\text{L mol}^{-1}) = 8.8$, which is consistent with Zn^{2+} retaining six-coordination in both complexes because of the smaller size of $\mathbf{2}^{2-}$.[15b]

The fluorescence intensity of the spectrum of [Zn(**3**)] derived from the fitting procedure applied to the data in Fig. 4 is slightly greater than that of [Zn(**3**)$_2$]$^{2-}$ (Fig. 5), which is consistent with a similar relationship for [Zn(**2**)] and [Zn(**2**)$_2$]$^{2-}$ [15b] and the broader observation that the fluorescence of $\mathbf{2}^{2-}$ in complexes of the general formula [Zn(**2**)L] varies significantly with the nature of L.[18] The fluorescence quantum yield, ϕ, of $\mathbf{3}^{2-}$ in [Zn**3**] is 0.14. The corresponding fluorescence spectra of (a) [Zn(**2**)]

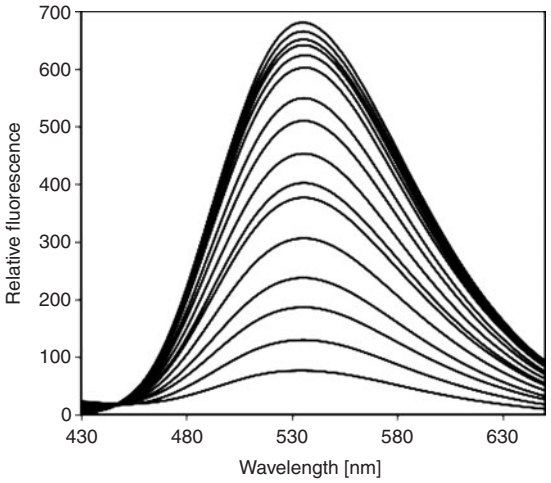

Fig. 4. Increase in fluorescence of 5.56×10^{-6} mol L^{-1} H**3**$^{-}$ in 25% v/v aqueous ethanol 0.10 mol L^{-1} in $NaClO_4$ buffered at pH 6.6 (1.0×10^{-3} mol L^{-1} NaPIPES) at 298.2 K with $[Zn^{2+}]_{total}$ in the range 3.9×10^{-7} mol L^{-1} ($= [Zn^{2+}]_{adventitious}$) to 5.0×10^{-5} mol L^{-1}. Excitation at 336 nm with excitation and emission slit widths of 5 mm.

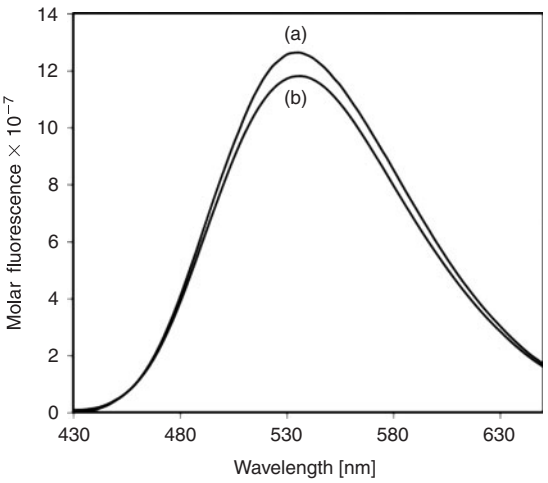

Fig. 5. The fluorescence spectra of (a) [Zn(**3**)] ($\lambda_{max} = 534$ nm and molar fluorescence $= 1.26 \times 10^8$ L mol^{-1}) and (b) [Zn(**3**)]$^{2-}$ per **3**$^{2-}$ ligand ($\lambda_{max} = 537$ nm and molar fluorescence $= 1.18 \times 10^8$ L mol^{-1}) derived from the fitting of an algorithm for the fluorescence variation with $[Zn^{2+}]_{total}$ and equilibria (1) and (2) as described in the text.

($\lambda_{max} = 483$ nm and molar fluorescence $= 5.56 \times 10^7$ L mol^{-1}) and (b) [Zn(**2**)]$^{2-}$ per **3**$^{2-}$ ligand ($\lambda_{max} = 483$ nm and molar fluorescence $= 6.17 \times 10^7$ L mol^{-1}) reflect their lesser conjugation through their shorter λ_{max}.[15a]

At the low $[H\mathbf{3}^-]_{total}$ and $[Zn^{2+}]_{total}$ of the fluorimetric study the low levels of impurity, or adventitious, $[Zn^{2+}]_{adventitious}$, arising dominantly from the $NaClO_4$ supporting electrolyte and the NaPIPES buffer become significant by comparison with the added $[Zn^{2+}]$ and were included in the $[Zn^{2+}]_{total}$ in the UV-vis and fluorimetric equilibrium studies.[15,19] The $[Zn^{2+}]_{adventitious}$ was determined in the 25% v/v aqueous ethanol 0.10 mol L^{-1} in $NaClO_4$ buffered at pH 6.6 (1.0×10^{-3} mol L^{-1} NaPIPES) in which all solutions for UV-vis and fluorometric studies were made. This determination was made using an EDTA titration method described in the experimental section, which shows the fluorescence of H**3**$^-$ to be negligibly low by comparison with those of [Zn(**3**)] and [Zn(**3**)]$^{2-}$ (Fig. 5). Under the conditions of the equilibrium studies $[Zn^{2+}]_{adventitious} = 3.9 \times 10^{-7}$ mol L^{-1}, which was added to the experimentally added $[Zn^{2+}]$ to give $[Zn^{2+}]_{total}$ used in the K_1 and K_2 fluorimetric and UV-vis determinations.

The absorbance spectrum of H**3**$^-$ in the absence of adventitious Zn^{2+} is shown in Fig. 3. Under the same conditions H**3**$^-$ shows no fluorescence. The fluorescence of **3**$^{2-}$ induced through coordination in [Zn(**3**)] and [Zn(**3**)]$^{2-}$ occurs through a chelation enhanced fluorescence (CHEF) mechanism,[28] whereby the coordination of the amide and quinoline nitrogens to Zn^{2+} forms a structurally stiffening five-membered chelate ring, which diminishes fluorescence quenching by energy dissipation through vibrational and rotational modes. The nitrogen coordination also decreases any residual photoinduced electron transfer effects.[29,30]

A qualitative UV-vis study shows that **3**$^-$ binds to Co^{2+}, Ni^{2+}, Cu^{2+}, and Cd^{2+} but not to Ca^{2+}, however, the complexes of the first three metals are not fluorescent probably due to quenching through electronic transitions occurring in their d^7, d^8, and d^9 manifolds. In contrast, the d^{10} Cd^{2+} complex, in which such quenching cannot occur, is fluorescent. However, in healthy cells the concentration of Cd^{2+} is very low by comparison with that of Zn^{2+} and so is unlikely to interfere significantly in the use of Zn^{2+} fluorophores in cellular and tissue studies.[31]

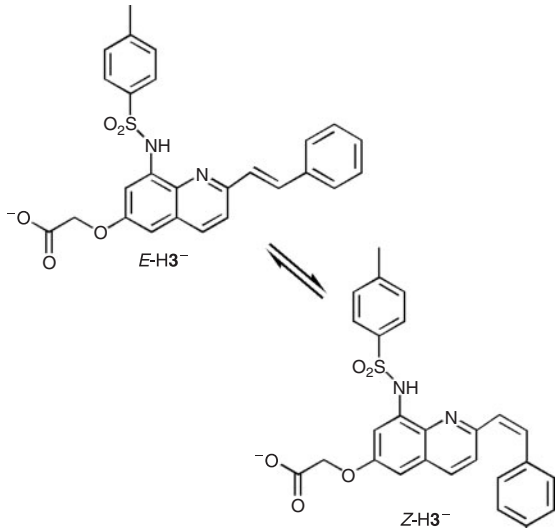

Fig. 6. Photoisomerization of *E*-H**3**$^-$ to *Z*-H**3**$^-$.

*Photoisomerism of H**3**$^-$*

A change in the solution spectrum of *E*-H**3**$^-$ occurs upon continuous exposure to laboratory light and is attributed to photoisomerization about the ethenyl bond to form *Z*-H**3**$^-$ (Fig. 6) as shown in Fig. 7. The small absorbance decrease is complete after 15 min when a photostationary state is reached in which the proportions of the *E*-H**3**$^-$ and *Z*-H**3**$^-$ isomers are unknown. This change reverses after refluxing in darkness with a catalytic amount of *p*-toluenesulfonic acid. To avoid any contribution to the above discussed UV-vis and fluorimetric equilibrium studies, all solution manipulation involving *E*-H**3**$^-$ was carried out under reduced light, and all solutions were contained in foil-wrapped vessels and allowed to equilibrate for at least 30 min at 298.2 K in darkness before spectroscopic measurement.

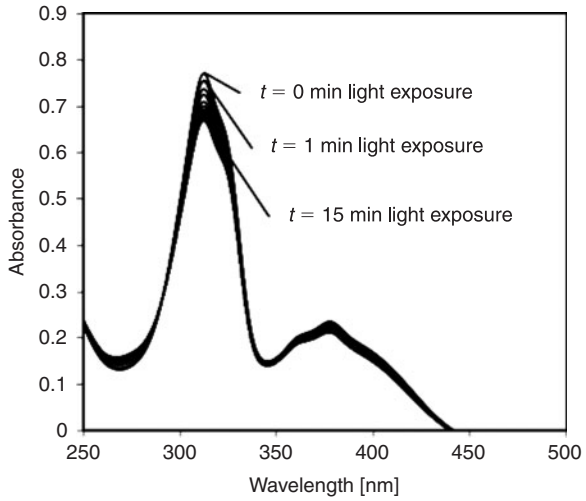

Fig. 7. The absorbance time dependence during exposure to daylight of *E*-H**3**$^-$ in 25% v/v aqueous ethanol 0.10 mol L^{-1} in $NaClO_4$ buffered at pH 6.6 (1.0×10^{-3} mol L^{-1} NaPIPES) at 298.2 K.

Conclusion

The K_1 value for [Zn(**3**)] is similar to that of [Zn(**2**)] while the K_2 value for [Zn(**3**)]$^{2-}$ is 200 times larger than that of [Zn(**2**)]$^{2-}$.[15b] This is consistent with the greater conjugation of **3**$^{2-}$ causing it to be a more effective bidentate Lewis base for Zn^{2+} than is **2**$^{2-}$. However, H_2**3** is not an ideal fluorophore for routine analytical use due to the photoisomerization of *E*-**3** to *Z*-**3** in solution in daylight unless care is taken to avoid it. Nevertheless, this study demonstrates the effect of increased conjugation in the quinoline-based fluorophores and provides insight for further Zn^{2+} selective fluorophore development.

Experimental

Materials

*Preparation of 2-((*E*)-2-Phenyl)ethenyl-8-(*N*-4-methylbenzenesulfonyl)aminoquinol-6-yloxyacetic Acid, H_2**3***

A solution of ethyl-2-(2-[(*E*)-2-phenyl-1-ethenyl]-6-quinolyloxy-8-*p*-toluenesulfonamido)acetate[27] (300 mg, 0.586 mmol) and sodium hydroxide (292 mg, 7.3 mmol) in ethanol (20 mL) was heated at reflux for 18 h. The mixture was cooled to room temperature and diluted with 10% w/v aqueous citric acid solution (20 mL). The precipitated solid was collected by vacuum filtration and washed with water (2 × 10 mL). The product crystallized from aqueous ethanol as pale orange needles (174 mg, 61%), mp 230°C (dec). ν_{max} (nujol)/cm^{-1} 3176 (b), 2582 (b), 1739 (s), 1625, 1600, 1596, 1504, 1209, 1162 (s), 1097, 960, 900, 858, 836, 690, 665. δ_H (d_6-DMSO) 9.9 (br s, 1H, NH), 8.15 (d, *J* 10.0, 1H, quinolyl H4), 7.87 (d, *J* 15.8, 1H, ethenyl H9), 7.84 (d, *J* 8.0, 2H, tosyl H2a, H2a′), 7.81 (d, *J* 10, 1H, quinolyl H3), 7.73 (d, *J* 7.6, 2H, styryl H11, H11′), 7.45 (d, *J* 15.8, 1H, ethenyl H10), 7.44 (d, *J* 7.6, 2H, styryl H12, H12′), 7.36 (m, 1H, styryl H13), 7.29 (d, *J* 8, 2H, tosyl H3a, H3a′), 7.26 (d, *J* 2.8, 1H, quinolyl H7), 6.77 (d, *J* 2.8, 1H, quinolyl H5), 4.75 (s, 2H, CH_2), 2.25 (s, 3H, CH_3). δ_C (d_6-DMSO) 169.7, 155.3, 152.4, 143.7, 136.5, 136.4, 135.7, 134.7, 133.8, 129.7, 128.9, 128.6, 128.3, 127.8, 127.1, 126.9, 121.1, 108.8, 101.9, 64.8, 20.9. Anal. Calc. for $C_{26}H_{22}N_2O_5S$: C 65.81, H 4.67, N 5.90. Found C 65.88, H 4.71, N 5.89%.

Other Materials

Sodium piperazine-*N*,*N*′-bis[2-ethanesulfonate] buffer, NaPIPES (Cal Biochem), NaOH (Ajax) and $HClO_4$ (70% in water, Ajax), and EDTA disodium salt ($Na_2EDTA{\cdot}H_2$) (Ajax), were used as received. Metal perchlorate salts were either purchased (Fluka) or prepared by reaction of the corresponding metal carbonate with a stoichiometric amount of perchloric acid. All perchlorates were recrystallized from ethanol/water, vacuum-dried, and stored over P_2O_5. Aqueous metal perchlorate solutions were standardized in triplicate by passing down a Dowex Ag 50W-X2 cation exchange resin (acid form) 2 × 20 cm column and back-titrating the acid in the collected eluent solution with aqueous NaOH solution. The NaOH solution was standardized against potassium phthalate. Quinine hemisulfate (Aldrich) was dried under vacuum at room temperature for 12 h and then stored over P_2O_5 before use in quantum yield determinations. Analytical grade ethanol was purified by fractional distillation under nitrogen. Deionized water was ultrapurified with a Milli-Q Reagent system to produce water with a specific resistance of >15 MΩ cm and then boiled to remove CO_2.

Glassware and instruments used in transferring, storing, preparing, and measuring the properties of the final product (including pipettes, cuvettes, and potentiometric titration cells) were thoroughly washed in Decon 90, rinsed several times, and then soaked overnight in Milli-Q water and oven-dried before use. Micropipettes (HTL) were used for all volume measurements under 2 mL.

Potentiometric Titrations

Potentiometric titrations were performed using a Metrohm 800 Dosino equipped with a 5 mL burette and an Orion Ross semi-micro combination pH electrode, which contained 0.10 mol L^{-1} $NaClO_4$ in 25% v/v aqueous ethanol. Data collection was controlled by the program Tiamo running off an IBM personal computer interfaced to the pH electrode through a 809 Titrando potentiometer. All titrations were thermostatted at 298.2 ± 0.1 K in a foil wrapped water-jacketed titration vessel that was closed to the atmosphere. Nitrogen was first bubbled through 0.10 mol L^{-1} KOH to remove CO_2 and then through 0.10 mol L^{-1} $NaClO_4$ to remove any KOH spray and to saturate it with solvent (25% v/v aqueous ethanol) before it was passed through the magnetically stirred titration solution before and during the titration.

All solutions were prepared in 25% v/v aqueous ethanol and were 0.10 mol L^{-1} in $NaClO_4$. Potentiometric titrations were performed by the titration of 2.0 mL aliquots of a solution containing ethyl-2-(2-[(*E*)-2-phenyl-1-ethenyl]-6-quinolyloxy-8-*p*-toluenesulfonamido)acetic acid, H_2**3** (1.03×10^{-3} mol L^{-1}), $HClO_4$ (9.21×10^{-3} mol L^{-1}), and $NaClO_4$ ($I = 0.1$ mol L^{-1}) with 0.126 mol L^{-1} NaOH (standardized by titration of 2 mL aliquots with 0.010 mol L^{-1} potassium phthalate). Calibrations were performed daily by titrating 2.0 mL of a 9.21×10^{-3} mol L^{-1} $HClO_4$ solution with standardized 0.126 mol L^{-1} NaOH, where both solutions were 0.10 mol L^{-1} in $NaClO_4$. An algorithm for the pH variation of a tribasic acid with added NaOH was fitted to the potentiometric data to derive the three pK_as using the Tiamo software.

Spectroscopic Measurements

All solutions for spectroscopic study were prepared in 25% v/v aqueous ethanol, 0.10 mol L^{-1} in $NaClO_4$ and 1.00×10^{-3} mol L^{-1} in NaPIPES buffer at pH 6.6. UV-vis spectra were recorded with a Varian Cary 300 spectrophotometer

using matched quartz cells with a path length of 1 cm in a cell block thermostatted at 298.2 ± 0.1 K. Samples were equilibrated for 10 min at this temperature before measurement. All spectra were obtained over a range of 250–450 nm with a slit width of 2 nm, a scan rate of 600 nm min^{-1} and a data collection interval of 1.0 nm.

Fluorescence spectra were recorded on a Varian Cary Eclipse fluorimeter. The solutions were contained in a 1 cm pathlength quartz cell and placed in a thermostatted 298.2 K sample block for 10 min before measurement. Spectra were obtained over a range of 430–650 nm with excitation at the isosbestic point at 336 nm (Figs 2 and 3). This isosbestic point was chosen as the excitation wavelength to ensure that any fluorescence changes were not due to differing absorbance characteristics of H**3**$^{-}$, [Zn**3**], and [Zn$\mathbf{3}_2$]$^{2-}$. The excitation and emission slit widths were 5 nm, the scan rate was 120 nm min^{-1} and the data collection interval was 1.0 nm. The quantum yields[32] were determined using quinine hemisulfate as the reference fluorophore and the refractive index of the solvent system was obtained from literature data.[33]

The K_1 and K_2 values were derived by fitting algorithms describing the variation of absorbance and fluorescence with equilibria (1) and (2) at 1 nm intervals over the ranges 270–450 nm and 430–650 nm, respectively, using the SPECFIT/32 protocol.[34]

The concentration of adventitious Zn^{2+} in 25% v/v aqueous/ethanol solutions 0.10 mol L^{-1} in $NaClO_4$ and 1.00×10^{-3} mol L^{-1} in NaPIPES buffer at pH 6.6 was determined by back titration with $Na_2EDTA{\cdot}H_2$ for which a Zn^{2+} complexation constant $K_1 = 10^{16.44}$ L mol^{-1} in aqueous solution is reported.[35] A series of solutions 5.56×10^{-6} mol L^{-1} in H**3**$^{-}$ was prepared in which [$Na_2EDTA{\cdot}H_2$] was gradually increased, and their fluorescence was determined over the range 430–650 nm with excitation at 336 nm. Fluorescence decreased with an increase in [EDTA] and extrapolation to zero fluorescence intensity yielded a value of 3.9×10^{-7} mol L^{-1}, which was also taken as the value of $[Zn^{2+}]_{adventitious}$ assuming stoichiometric 1:1 complexation of Zn^{2+} by $EDTA^{4-}$.

Accessory Publication

Fig. A1 shows the potentiometric titration curve for $H_3\mathbf{3}^+$ and the best-fit curve; Fig. A2 shows the speciation of $H_3\mathbf{3}^+$, $H_2\mathbf{3}$, H**3**$^{-}$, and **3**$^{2-}$ with pH; Fig. A3 shows the increase in absorbance as $[Zn^{2+}]_{total}$ increases and the best fit curve; Fig. A4 shows the increase in fluorescence as $[Zn^{2+}]_{total}$ increases and the best fit curve; and Fig. A5 shows the speciation of $H_2\mathbf{3}$, [Zn(**3**)], and [Zn$(\mathbf{3})_2$]$^{2-}$ derived from the fluorescence data. All figures are available on the Journal's website.

Acknowledgements

The award of an Australian Postgraduate award to H. Coleman and funding of this research by the University of Adelaide is gratefully acknowledged. We thank Dr D.-T. Pham, Ms. C. Baker, and Dr J. Cawthray for their helpful input.

References

[1] C. F. Mills, *Zinc in Human Biology* **1989** (Springer-Verlag: London).
[2] J. R. R. Fausto da Silva, R. J. P. Williams, *The Biological Chemistry of the Elements* **1992** (Oxford University Press: Oxford).
[3] B. L. Vallee, D. S. Auld, *Acc. Chem. Res.* **1993**, *26*, 543. doi:10.1021/AR00034A005
[4] E. Kimura, *Acc. Chem. Res.* **2001**, *34*, 171. doi:10.1021/AR000001W
[5] C. Andreini, L. Banci, I. Bertini, A. Rosato, *J. Proteome Res.* **2006**, *5*, 3173. doi:10.1021/PR0603699
[6] D. H. Nies, *Science* **2007**, *317*, 1695. doi:10.1126/SCIENCE.1149048
[7] E. L. Que, D. W. Domaille, C. J. Chang, *Chem. Rev.* **2008**, *108*, 1517. doi:10.1021/CR078203U
[8] W. Maret, Y. Li, *Chem. Rev.* **2009**, *109*, 4682. doi:10.1021/CR800556U
[9] A. Nomura, Y. Sugiura, *J. Am. Chem. Soc.* **2004**, *126*, 15374. doi:10.1021/JA045663L
[10] M. Nagaoka, Y. Doi, J. Kuwahara, Y. Sugiura, *J. Am. Chem. Soc.* **2002**, *124*, 6526. doi:10.1021/JA025856D
[11] C. I. Stains, J. R. Porter, A. T. Ooi, D. J. Segal, I. Ghosh, *J. Am. Chem. Soc.* **2005**, *127*, 10782. doi:10.1021/JA051969W
[12] M. P. Cuajungco, G. J. Lees, *Neurobiol. Dis.* **1997**, *4*, 137. doi:10.1006/NBDI.1997.0163
[13] L. E. Scott, C. Orvig, *Chem. Rev.* **2009**, *109*, 4885. doi:10.1021/CR9000176
[14] M. Nolan, S. J. Lippard, *Acc. Chem. Res.* **2009**, *42*, 193. doi:10.1021/AR8001409
[15] (a) K. M. Hendrickson, T. Rodopoulos, P.-A. Pittet, I. Mahadevan, S. F. Lincoln, A. D. Ward, T. Kurucsev, P. A. Duckworth, I. J. Forbes, P. D. Zalewski, W. H. Betts, *J. Chem. Soc., Dalton Trans.* **1997**, 3879. doi:10.1039/A703433D
(b) K. Hendrickson, *PhD Thesis: The use and spectroscopic properties of Zinquin, a zinc(II) specific fluorophore* **1999** (University of Adelaide: Adelaide).
[16] S. C. Burdette, C. J. Frederickson, W. Bu, S. J. Lippard, *J. Am. Chem. Soc.* **2003**, *125*, 1778. doi:10.1021/JA0287377
[17] T. Hirano, K. Kikuchi, Y. Urano, T. Nagano, *J. Am. Chem. Soc.* **2002**, *124*, 6555. doi:10.1021/JA025567P
[18] K. M. Hendrickson, J. P. Geue, O. Wyness, S. F. Lincoln, A. D. Ward, *J. Am. Chem. Soc.* **2003**, *125*, 3889. doi:10.1021/JA020685Y
[19] S. G. Schulman, L. B. Sanders, *Anal. Chim. Acta* **1971**, *56*, 83. doi:10.1016/S0003-2670(01)80111-2
[20] P. D. Zalewski, I. J. Forbes, W. H. Betts, *Biochem. J.* **1993**, *296*, 403.
[21] P. D. Zalewski, I. J. Forbes, R. F. Seamark, R. Borlinghaus, W. H. Betts, S. F. Lincoln, A. D. Ward, *Chem. Biol.* **1994**, *1*, 153. doi:10.1016/1074-5521(94)90005-1
[22] P. Coyle, P. D. Zalewski, J. C. Philcox, I. J. Forbes, A. D. Ward, S. F. Lincoln, I. Mahadevan, A. M. Rofe, *Biochem. J.* **1994**, *303*, 781.
[23] P. D. Zalewski, S. H. Millard, I. J. Forbes, O. Kapaniris, A. Slavotinek, W. H. Betts, A. D. Ward, S. F. Lincoln, I. Mahadevan, *J. Histochem. Cytochem.* **1994**, *42*, 877.
[24] P. D. Zalewski, X. Jian, L. L. L. Soon, W. G. Breed, R. F. Seamark, S. F. Lincoln, A. D. Ward, F.-Z. Sun, *Reprod. Fertil. Dev.* **1996**, *8*, 1097. doi:10.1071/RD9961097
[25] I. B. Mahadevan, M. C. Kimber, S. F. Lincoln, E. R. T. Tiekink, A. D. Ward, W. H. Betts, I. J. Forbes, P. D. Zalewski, *Aust. J. Chem.* **1996**, *49*, 561.
[26] P. Zalewski, A. Truong-Tran, S. F. Lincoln, A. D. Ward, A. Shankar, P. Coyle, L. Jayaram, A. Copley, D. Grosser, C. Murgia, C. Lang, R. Ruffin, *Biotechniques* **2006**, *40*, 509. doi:10.2144/06404RR02
[27] M. C. Kimber, I. B. Mahadevan, S. F. Lincoln, E. R. T. Tiekink, *J. Org. Chem.* **2000**, *65*, 8204. doi:10.1021/JO000678X
[28] A. W. Czarnik, *Acc. Chem. Res.* **1994**, *27*, 302. doi:10.1021/AR00046A003
[29] D. G. Whitten, *Acc. Chem. Res.* **1980**, *13*, 83. doi:10.1021/AR50147A004
[30] M. R. Wasielewski, *Chem. Rev.* **1992**, *92*, 435. doi:10.1021/CR00011A005
[31] M. Schmid, S. Zimmermann, H. F. Krug, B. Sures, *Environ. Int.* **2007**, *33*, 385. doi:10.1016/J.ENVINT.2006.12.003
[32] W. H. Melhuish, *J. Phys. Chem.* **1961**, *65*, 229. doi:10.1021/J100820A009
[33] *Handbook of Chemistry and Physics* (Eds R. C. Weast, S. M. Selby) **1977** (CRC Press: Cleveland, OH).
[34] R. A. Binstead, B. Jung, A. D. Zuberbuhler, *SPECFIT/32, v3.0.39(b)* **2007** (Spectrum Software Associates: Marlborough, MA).
[35] R. M. Smith, A. E. Martell, *Critical Stability Constants, Vol. 2: Amines* **1975** (Plenum Press: New York, NY).